Catal Lett (2008) 120:56–64
DOI 10.1007/s10562-007-9249-8

Phenol Hydroxylation Using Fe/Al-MCM-41 Catalysts

M. Esther Leena Preethi · S. Revathi · T. Sivakumar · D. Manikandan · D. Divakar · A. Valentine Rupa · M. Palanichami

Received: 6 July 2007 / Accepted: 17 August 2007 / Published online: 11 September 2007

Abstract Fe loaded Al-MCM-41, (Si/Al = 25, 50, 75 and 100) catalysts were synthesized by hydrothermal method and characterized by the XRD, BET (surface area), FT-IR, and UV- vis and Mössbauer techniques. The liquid phase hydroxylation of phenol with hydrogen peroxide was studied and exclusive formation of dihydroxybenzene was observed. The phenol conversion was found to be almost same at various reaction temperatures viz 40, 60 and 80 °C, but at room temperature only about 30% conversion was recorded. The activity followed the order Fe/Al-MCM-41 (25) > Fe/Al-MCM-41(50) > Fe/Al-MCM-41 (75) > Fe/Al-MCM-41 (100) which was also the order of acidity. Effects of Fe content in Fe/Al-MCM-41 catalysts, solvent, phenol/H_2O_2 mole ratio on phenol conversion was examined. The reaction was also carried out over 10% iron loaded mordenite and the results are compared.

Keywords Phenol · Hydrogen peroxide · Hydroxylation · MCM-41 · Iron

M. Esther Leena Preethi · S. Revathi · T. Sivakumar (✉) · D. Manikandan · D. Divakar · A. Valentine Rupa
Catalysis Lab, Department of Chemical Engineering, A.C. College of Technology, Anna University, Chennai 600 025, India
e-mail: sivakumar@annauniv.edu

M. Palanichami
Department of Chemistry, College of Engineering, Anna University, Chennai 600 025, India

1 Introduction

Hydroquinone and catechol, the products of phenol hydroxylation, find their applications in the multifaceted angle of industrial synthesis as antioxidants, polymerization inhibitors, photography chemicals and are also used as intermediates in agrochemical and fine chemical industries [1–3]. Therefore much attention has been paid in the production of these dihydroxy compounds through catalytic route. Iron containing microporous and mesoporous molecular sieves show redox properties which characterize them as suitable catalysts for phenol hydroxylation reaction as iron shows better activity than other transition metals [4–11] but the expected result has been eschewed by the pore size constraint posed by the microporous support materials. Since the discovery of mesoporous silicates by Mobil Oil researcher, MCM-41 and MCM-48 materials have been most often studied as supports for various transition metals [12, 13]. In the past, hydroxylation of phenol has been carried over different mesoporous materials viz surface functionalized MCM-41 [14], Fe-HMS [15] CuO-containing MCM-48 [16] and Fe-MCM-41 [17] catalysts. But no such work has been carried out over Fe/Al-MCM-41. Introduction of iron into the mesoporous material by wet impregnation technique exploits most of its redox property than tetrahedrally coordinated Fe^{3+} located in the skeleton of the materials in which iron was introduced during the synthesis [18]. The wet impregnated Al-MCM-41 with iron salts was found to be the most effective catalyst in the sulfurisation of methanol when compared with purely siliceous MCM-41 [19]. In the present work Fe impregnated Al-MCM-41 with various Si/Al ratio were prepared characterized and the catalytic activity were tested towards phenol hydroxylation. The parameters such as temperature, mole ratio, solvents

influencing the reaction were studied and a possible reaction mechanism was also proposed.

2 Experimental

2.1 Materials

Sodium metasilicate ($Na_2SiO_3 \cdot 5H_2O$), aluminium sulfate ($Al_2SO_4 \cdot 18H_2O$), cetyltrimethylammoniumbromide ($C_{16}H_{33}$ $(CH_3)_2N^+Br^-$), sulfuric acid (H_2SO_4), iron (III) nitrate, phenol and hydrogen peroxide. All the chemicals were of AR grade and purchased from Aldrich & Co., USA.

2.2 Commercial Catalytic Materials

Sodium form of commercial zeolite Mordenite (MOR) with $SiO_2/Al_2O_3 = 12$ was purchased from United Catalysts Ltd., India. The surface area of the material used was 583 m^2/g.

2.3 Synthesis of Al-MCM-41

The Al-MCM-41 (Si/Al ratios: 25, 50, 75 and 100) molecular sieves, were synthesized as reported elsewhere [12, 20] using hydrothermal method with the gel composition of SiO_2:xAl_2O_3:0.2CTAB:0.89H_2SO_4:120H_2O. Sodium meta silicate was used as the silicon source, cetyltrimethylammonium bromide (CTAB) as the structure directing agent and aluminium sulphate as the aluminium source. Sodium meta silicate (21.21 g) was dissolved in 80 mL of water and the mixture was stirred for half an hour. Then the required quantity of aluminium sulphate, dissolved in 15 mL of water, was added and stirred for 1 h. Then 40 mL of 4 N sulphuric acid was added drop by drop until the gel formed. The stirring was continued for 2 h. Exactly 7.28 g of CTAB, dissolved in 25 mL of water was added and stirring was continued for a further 2 h. Then the gel was transferred in to an autoclave and was kept in an air oven at 145 °C for 36 h. Then the product obtained was filtered, washed several times with double distilled water and dried at 80 °C in an air oven for 2 h. Then the sample was calcined in a muffle furnace at 550 °C for 6 h to remove the template. The sample calcined by this procedure was ion exchanged repeatedly with one molar solution of ammoniumnitrate and then filtered, dried and calcined again at 550 °C for 12 h in nitrogen atmosphere.

2.4 Wet Impregnation

The wet impregnation was carried out as reported elsewhere [21]. The above calcined mesoporous materials was flooded with the appropriate amount (a large volume of the initial solution which was reduced on drying) of an aqueous solution of iron (III) nitrate containing 10 wt% of iron and mixed. Then the mixture was heated at ~80 °C, without stirring, for 8 h and water present was evaporated under stirring at ~80 °C. The obtained powder was dried at 60 °C and then calcined at 550 °C for 4 h in a muffle furnace.

2.5 Catalytic Runs

The phenol hydroxylation was carried out at 40 °C under batch reaction conditions using magnetically stirred 50 mL glass reactor fitted with a reflux condenser, a thermometer and a septum for withdrawing the product samples. A typical reaction mixture in the reactor contained phenol (0.05 mol), hydrogen peroxide (0.15 mol) and a freshly activated catalyst (0.1 g). After the reaction was over, activation of the catalyst was done by calcination at 500 °C in air for 5 h.

2.6 Analysis

The progress of the reaction was monitored by sampling periodically and analyzed using gas chromatograph (Shimadzu 9A) equipped with flame ionization detector fitted with 5% SE 30 column (2 m length). The product analyzed by GC revealed the exclusive formation of hydroquinone and catechol.

2.7 Characterization

The powder X-ray diffraction patterns were recorded for the synthesized catalyst by using a Siemens D5005 Stereo scan diffractometer with nickel filtered Cu KN radiation (operating at 40 kV and 30 mA) source and a liquid nitrogen-cooled germanium solidstate detector. The diffractograms were recorded in the two, range 0.8–10° in steps of 0.02 with a count time of 10 s at each point. Surface area, pore volume and pore size distribution were measured by nitrogen adsorption at –196 °C using an ASAP-2010 porosimeter from Micromeritics Corporation, GA. The samples were degassed at 350 °C and 10^{-5} Torr overnight prior to the adsorption experiments. The mesopore volume was estimated from the amount of nitrogen adsorbed at a relative pressure of 0.5 by assuming that all the mesopores were filled with condensed nitrogen in the normal liquid state. Pore size distribution was estimated using the Barrett, Joyner and Halenda (BJH) algorithm (ASAP-2010) available as built-in software from Micromeritics. The acidity of the materials was analysed by pyridine adsorption and characterized by using FT-IR. The catalyst sample was finely ground and pressed into a self supporting wafer.

The wafers were calcined under vacuum at 500 °C for 2 h, followed by exposure of pyridine vapour. The wafers were allowed to adsorb pyridine for 1 h. The thin wafer was placed in the FT-IR cell and the spectrum was recorded on a Nicolet 800 (Avatar 360) FT-IR spectrophotometer. The diffuse reflectance UV-Vis spectra were recorded in the wavelength range of 200–800 nm with Shimadzu UV-2101PC spectrometer equipped with a diffuse reflectance attachment using solid sample holder. Quantitative EDS microanalyses were made in an SEM (JEOL 5800 LV) with a PGT Prism detector and an IMIX processing and quantification software. The SEM operating conditions were 15 kV, beam current 1 nA. ^{27}Fe Mössbauer spectra were measured on a constant acceleration spectrometer in a triangular mode with a ^{27}Co:Rh source. Mössbauer spectra were recorded for Fe/Al-MCM-41 (50) at 27 °C. The overall spectra were deconvoluted with calculated Mossbauer spectra that consisted of Lorentzian shape lines.

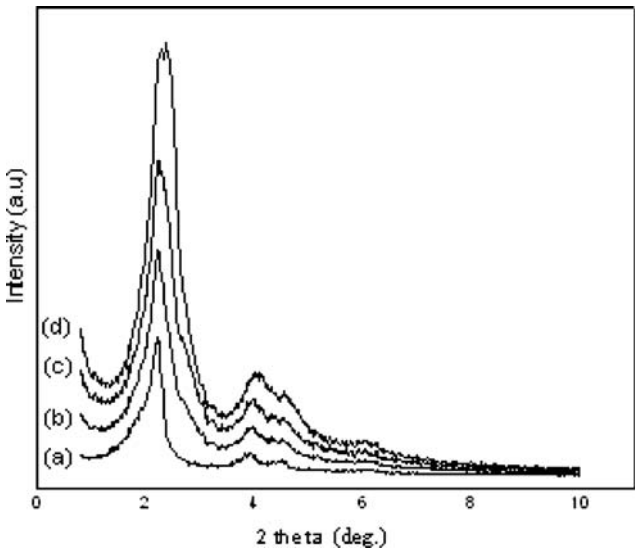

Fig. 1 XRD patterns of calcined (**a**) Fe/Al-MCM-41 (25), (**b**) Fe/Al-MCM-41 (50), (**c**) Fe/Al-MCM-41 (75) and (**d**) Fe/Al-MCM-41 (100)

3 Results and Discussion

3.1 Characterization of Fe/Al-MCM-41

3.1.1 XRD

Figure 1 displays the XRD patterns of calcined Fe/Al-MCM-41 (25), Fe/Al-MCM-41 (50), Fe/Al-MCM-41 (75) and Fe/Al-MCM-41 (100). An intensive peak observed at $2\alpha = 2.2–2.4°$ for all the four samples corresponds to the (100) reflection peak [22]. As Si/Al ratio of Al-MCM-41 in Fe impregnated Al-MCM-41 catalyst increased the d-spacing and the lattice parameter also slightly increased (Table 1). This can be explained based on the hydrophilic and hydrophobic properties of Al-MCM-41 as described by Climent et al. [23] where it describes as the increase of aluminium content increases hydrophilic property of the Al-MCM-41. Although the quantity of iron loading is amounted to be the same over all the synthesized catalysts, due to the comparatively high hydrophilicity of Al-MCM-41 [24] more of Fe^{3+} precursor can enter inside the pores and has been incorporated inside the framework as evident by the higher d spacing and lattice parameter values [15]. Because the ionic radius of Fe^{3+} (0.064 nm) is larger than the radius of Si^{4+} (0.026 nm).

3.1.2 N_2 Adsorption Isotherm

The BET surface area, pore size and pore volume for calcined materials are presented in Table 1. As the Si/Al ratio of Fe/Al-MCM-41 catalysts increases the surface area, pore size and pore diameter value also increases. The nitrogen adsorption–desorption isotherms of calcined Fe/Al-MCM-41 (25), Fe/Al-MCM-41 (50), Fe/Al-MCM-41 (75), and Fe/Al-MCM-41 (100) are shown in Fig. 2. All of them exhibit isotherms of type IV featuring a step at a relative pressure of $0.25 < p/p_0 < 0.35$ due to capillary condensation of N_2 in the primary mesopores. The absence of hysteresis loop in the desorption branch suggests that no interparticle mesoporosity is present. The pore size distribution for calcined materials is shown in Fig. 3. The observed results are similar to those reported in the literature [25].

3.1.3 Acidity Analysis

The acidity of the calcined materials was measured by pyridine adsorption followed by FT-IR analysis and the FTIR spectra are given in Fig. 4. The samples show band due to Lewis acid bound (1450, 1575 and 1623 cm^{-1}), Bronsted acid bound (1545 and 1640 cm^{-1}) and both Lewis and Bronsted acid bound pyridine (1490 cm^{-1}). These data coincide with those reported by Climent et al. [24]. The acidity of the catalysts was calculated using the extinction coefficients of the bands of Bronsted and Lewis acid site adsorbed pyridine [26] and the results are presented in Table 2. Both Lewis and Bronsted acidities decreased with increase in Si/Al ratio. Among the catalysts synthesized, Fe/Al-MCM-41 (25) found to have the highest acidity.

3.1.4 DRS UV–Vis Spectroscopy

The diffuse reflectance UV-visible spectrum was recorded for calcined Fe/Al-MCM-41 (100) catalyst in order to identify the metal ion co-ordination and its existence in the

Table 1 Physiochemical properties of catalysts

Sample	d_{100} (Å)	a_0^a (nm)	Pore size (nm)	Wall thickness[b] (nm)	S_{BET} ($m^2\ g^{-1}$)	Pore volume ($cm^3\ g^{-1}$)
Fe/Al-MCM-41 (25)	46.98	5.4249	2.562	2.8629	620.8	0.2365
Fe/Al-MCM-41 (50)	46.95	5.4214	2.576	2.8454	646.6	0.2412
Fe/Al-MCM-41 (75)	44.72	5.1639	2.591	2.5729	688.0	0.2871
Fe/Al-MCM-41 (100)	43.52	5.0254	2.612	2.4134	694.0	0.3270

[a] $a_0 = 2d_{100}/\sqrt{3}$

[b] The wall thickness was calculated by subtracting the pore size from the unit cell parameter (a_0)

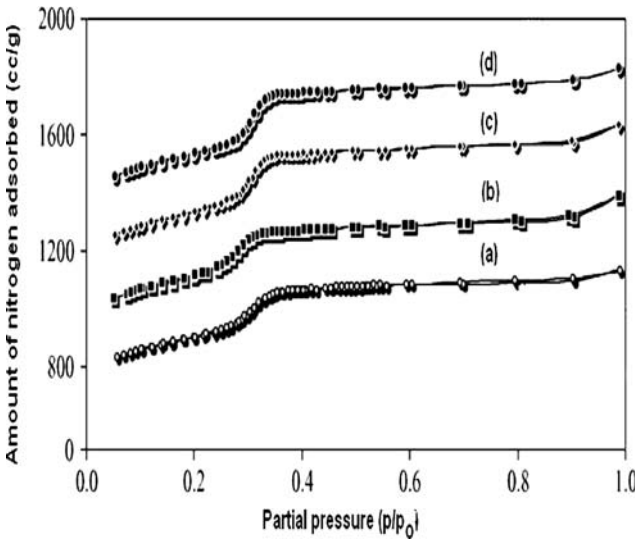

Fig. 2 The nitrogen adsorption-desorption isotherms of calcined catalysts (**a**) Fe/Al-MCM-41 (25), (**b**) Fe/Al-MCM-41 (50), (**c**) Fe/Al-MCM-41 (75) and (**d**) Fe/Al-MCM-41 (100)

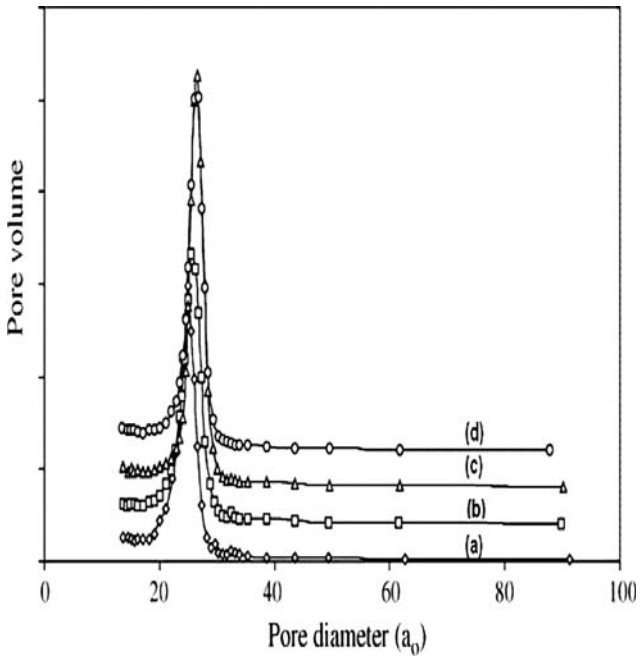

Fig. 3 The pore size distribution of calcined catalysts (**a**) Fe/Al-MCM-41 (25), (**b**) Fe/Al-MCM-41 (50), (**c**) Fe/Al-MCM-41 (75) and (d) Fe/Al-MCM-41 (100)

framework or extra framework position in the modified molecular sieves (Fig. 5). Two bands, at around 226 and 245 nm were observed in all the studied samples. These bands are usually assigned to the $t_1 \rightarrow t_2$ and $t_1 \rightarrow e$ transitions involving Fe^{3+} in $[FeO_4]$ tetrahedral coordination [27–29]. Octahedral complexes of Fe^{3+} are also characterized by two strong DR-UV bands in the 200–300 nm region [30, 31]. According to the literature, CT bands between 300 nm and 400 nm are assigned to octahedral Fe^{3+} in small oligomeric Fe_xO_y clusters [31].

3.1.5 Mössbauer Analysis

The Mössbauer spectrum of Fe/Al-MCM-41 (25), taken at room temperature, is shown in Fig. 6, and the data is listed in Table 3. The doublet lines and Mössbauer parameters of the samples are indicative of high spin paramagnetic Fe^{3+} species in the MCM-41 material. It was reported that Fe^{3+} species give the isomer shift (IS) <0.3 mm s^{-1} in the tetrahedral coordination and >0.3 mm s^{-1} in the octahedral co-ordination [32]. The figure illustrates two types of spectra for Fe/Al-MCM-41 (25), one with quadrupole splitting and the other without quadrupole splitting. This concludes that some of the Fe^{3+} enters the framework during the process of impregnation and the remaining exist as non-framework Fe^{3+} clusters in the mesopores. Since Fe^{3+} in the framework carries symmetrical electron distribution in its valence shell ($3d^5$), and symmetrical tetrahedral oxide sites, it is expected to give Mössbauer spectrum without any quadrupole splitting. Therefore, the one with quadrupole splitting is assigned to non-framework iron oxide. Based on the intensity of these two spectra the percentage of frame work iron and nonframe work iron have been calculated and found to be 15% and 85 % respectively.

3.1.6 SEM-EDS Analysis

The elemental content in Fe/Al-MCM-41 for various Si/Al ratios (25, 50, 75 and 100) were recorded using

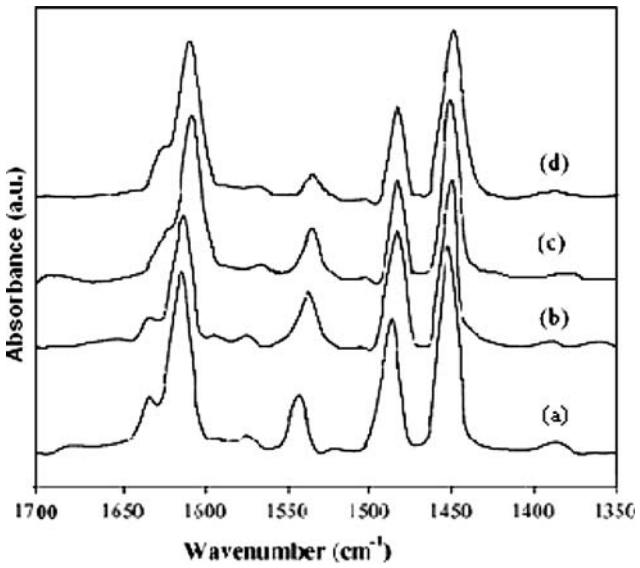

Fig. 4 The FT-IR spectra of pyridine adsorbed catalysts (**a**) Fe/Al-MCM-41 (25), (**b**) Fe/Al-MCM-41 (50), (**c**) Fe/Al-MCM-41 (75) and (**d**) Fe/Al-MCM-41 (100)

Table 2 Bronsted and Lewis acidity values of synthesized mesoporous materials

Catalyst	Bronsted acidity[a]	Lewis acidity[a]
Fe/Al-MCM-41 (25)	9.0	11.8
Fe/Al-MCM-41 (50)	8.3	11.6
Fe/Al-MCM-41 (75)	4.8	9.1
Fe/Al-MCM-41 (100	4.7	8.2

[a] Acidity (μmolpy/g catalyst); Temperature = 150 °C

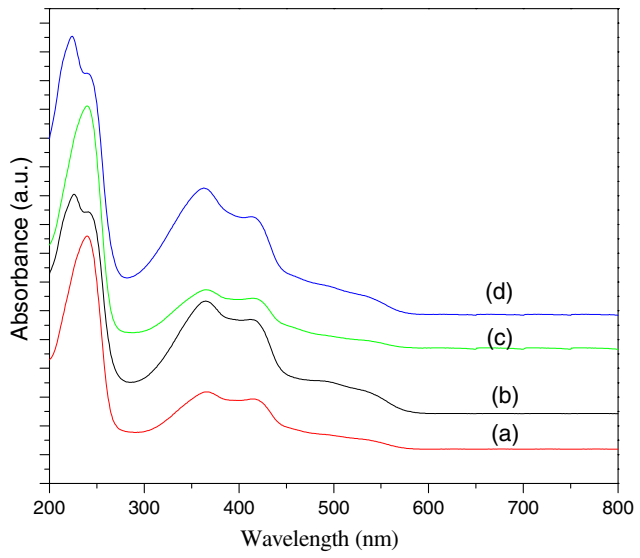

Fig. 5 The diffuse reflectance spectra of (**a**) Fe/Al-MCM-41 (25), (**b**) Fe/Al-MCM-41 (50), (**c**) Fe/Al-MCM-41 (75) and (**d**) Fe/Al-MCM-41 (100)

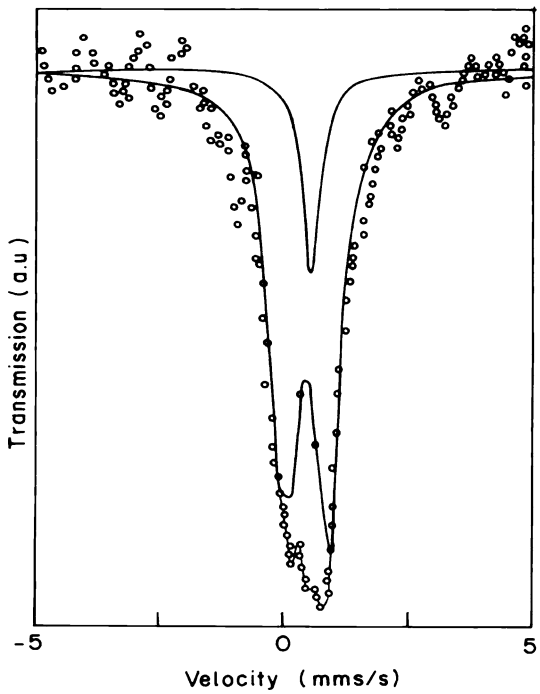

Fig. 6 Mössbauer spectrum of Fe/Al-MCM-41 (25)

Table 3 Mössbauer parameters of the Fe/Al-MCM-41 (50) catalysts

Isomer shift, IS (mm s^{-1})	Quadrupole splitting, QS (mm s^{-1})	Line-width (mm s^{-1})	Spectral contribution (%)
0.34	0.98	0.74	85
0.19	0.00	0.49	15

SEM-EDS. The results of the percentage elemental composition of iron and Si/Al ratios of the materials are given in Table 4. The synthesized catalysts contain a slightly higher Si/Al ratio. The elemental weight percentage of the impregnated iron remained almost the same (10 wt%) in all the samples.

3.2 Catalytic Activity Studies

3.2.1 Effect of Mole Ratio

The effect of mole ratio on phenol conversion was studied over highly acidic Fe/Al-MCM-41 (25) catalyst with varying amounts of hydrogen peroxide to a fixed amount of phenol from 1:1 to 1:5 (phenol: H_2O_2) ratios at 40 °C and the results are presented in Fig. 7. The phenol conversion increased when the mole ratio increased from 1:1 to 1:3 and thereafter levelled off. The decrease in conversion of phenol when the mole ratio increased from 1:3 to 1:5 may be due to more chemisorptions of H_2O_2 and less

Table 4 Phenol hydroxylation with hydrogen peroxide over Fe/Al-MCM-41 catalysts and Fe/MOR zeolite[a]

Catalysts	Si/Al ratio		Fe[b] (Element %)	Conv. of phenol (wt%)	TOF[c] (10^{-4} s^{-1} mol^{-1} Fe)	P.D. (wt%)[d]	
	Gel ratio	EDS				CH[e]	HQ[f]
Fe/Al-MCM-41 (25)	25	27	10.00	58.50	14.9313	38.92	61.06
Fe/Al-MCM-41 (50)	50	53	9.97	55.32	14.7356	39.56	60.44
Fe/Al-MCM-41 (75)	75	76	9.94	50.48	14.4781	41.68	58.32
Fe/Al-MCM-41 (100)	100	104	10.00	41.87	14.1246	45.29	54.71
Fe/MOR	12	14	10.00	20.67	0.2598	100.00	–

[a] Reaction condition: Catalyst(g) = 0.1 g; phenol (mol) = 1; hydrogen peroxide (mol) = 3; hydrogen peroxide/phenol (molar ratio) = 3; reaction temperature (K) = 40 °C reaction time (h) = 4

[b] Elemental composition of iron in percentage as analysed by SEM-EDS

[c] Turnover rates are expressed as turnover frequency(TOF, moles of phenol converted s^{-1} mol^{-1} Fe)

[d] Product distribution in weight percentage

[e] Catechol

[f] Hydroquinone

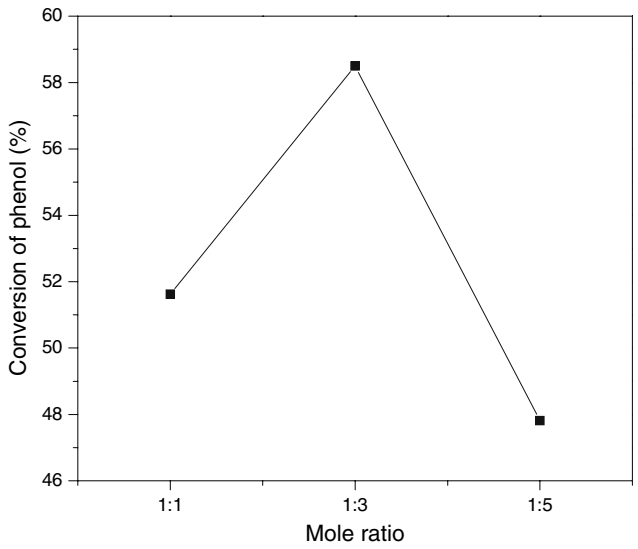

Fig. 7 Effect of mole ratio (phenol: H_2O_2) on phenol conversion over Fe/Al-MCM-41 (25)

chemisorption of phenol on the active sites. Hence from this study it was concluded that the mole ratio 1:3 (phenol: H_2O_2) would be the optimum one. Therefore further studies with different catalysts have been carried out with this optimized mole ratio (1:3).

3.2.2 *Phenol hydroxylation reactions over Fe/Al-MCM-41 (25), Fe/Al-MCM-41 (50), Fe/Al-MCM-41 (75) andFe/Al-MCM-41 (100) catalysts*

Phenol hydroxylation with hydrogen peroxide over all the catalysts was carried at 40 °C for 4 h in the liquid phase with phenol and hydrogen peroxide with molar ratio of 1:3 using 0.1 g catalyst and the results are presented in Table 4. Hydroquinone and catechol are formed in the liquid phase, No black tarry material and benzoquinone was detected as repeated elsewhere [3, 17, 33–35] respectively. No induction period was observed with Fe containing Al-MCM-41 catalysts whereas Fe species in the MCM-41 framework seem to require more energy than that of Fe ions to generate OH radicals from H_2O_2 and the phenol hydroxylation proceeded more slowly with an induction period [17]. Effects of various reaction parameters on phenol hydroxylation were studied and the experimental findings were interpreted based on the redox mechanism proposed.

The phenol conversion, turn over frequency and product selectivity is given in Table 4. Hydroxylation of phenol has been known to proceed by a redox mechanism [17]. Although the quantity of iron is same over all the synthesized catalysts (Table 4), slight variation in the percentage conversion of phenol (4–10%) was observed which may be due to variation in Si/Al ratio. Thus Fe/Al-MCM-41 (25) showed highest activity among the catalyst tested. Fe/MOR showed least activity in this reaction. This may be due to diffusion constrain for the reactants to pass in to the pores of MOR. The selectivity of the products towards hydroquinone is higher than catechol over all the mesoporous catalyst under investigation except for Fe-MOR. Based on the conversion and hydroquinone selectivity, Fe/Al-MCM-41 (25) was found to be the best catalyst.

3.2.3 *Mechanism*

Higher selectivity to hydroquinone over all Fe/Al-MCM-41 catalysts suggests preferential adsorption of H_2O_2 on Fe^{3+} site leaving more phenol in the unadsorbed state which is a

requirement for selective parahydroxylation. Choi et al. [17] studied the same reaction over Fe-MCM-41 and iron oxide impregnated MCM-41. Though they were able to show high conversion the selectivity of the products was reversed. Hydroquinone selectivity was lower than catechol. Fe/Al-MCM-41 being hydrophilic than MCM-41 favors both chemisorptions of hydrogen peroxide and phenol on the active site. Owing to polarity factor the much polar and relatively small sized hydroxyl radical is preferentially chemisorbed and the reaction between free phenol and hydroxyl radical might yield more selective hydroquinone. Since the molar ratio of investigation contains comparatively excess amount of hydrogen peroxide which inherits 30% of water in it, the hydroxyl group of phenol would be surrounded with water and hence para hydroxylation is much favored under the specified reaction condition. Thermodynamically more favored catechol formation is possible when both phenol and hydrogen peroxide adsorb on the same active site as described by reaction Scheme 1.

Iron oxide impregnated in Al-MCM-41 catalysts are better than all the previously reported catalysts because the strong adsorption of phenol and dihydroxy benzenes on Lewis acid site which can lead to coke formation and further undesired reaction like formation of tarry product and benzoquinone is being prohibited by the structure and the chemical characteristics of the catalyst used as evident from the experimental observation.

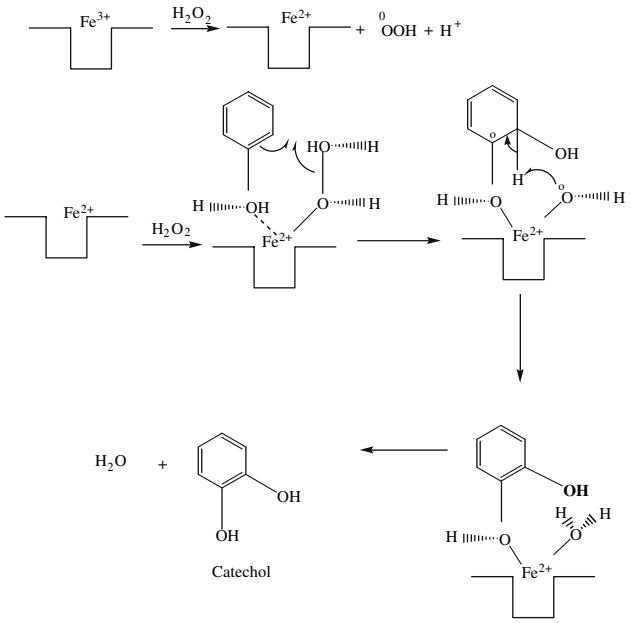

Scheme 1

3.2.4 *Effect of Time on Stream on Conversion at Different Temperatures*

The effect of time on stream on conversion at different temperatures over Fe/Al-MCM-41 (25) was also studied and the data is presented in Fig. 8. The results show that the lower temperatures were better than the higher ones. As shown in the figure almost no induction period was observed even at lower temperature. Less conversion at higher temperatures was attributed to decomposition of H_2O_2. At 20 °C, conversion was very low. It might be due to association of H_2O_2 that suppressed chemisorptions. Hence 40 °C becomes the optimum one for the hydroxylation of phenol. The noticeable conversion even at lower temperature is due to the redox transition of iron in the catalyst.

3.2.5 *Effect of Solvent*

Figure 9 shows that the conversion of phenol was strongly dependent on the solvent used [36]. The result shows that water is the best solvent for the hydroxylation of phenol using Fe/Al-MCM-41 (25). The solubility of hydrogen peroxide is lower in organic solvent, which suppresses the dissociation of hydrogen peroxide making it more difficult to approach the active site (Fe^{3+}) and hence as observed, the rate of the reaction is slow. When water was used as the solvent hydrogen peroxide reacts easily to form OH^- radical which can rapidly diffuse in the medium.

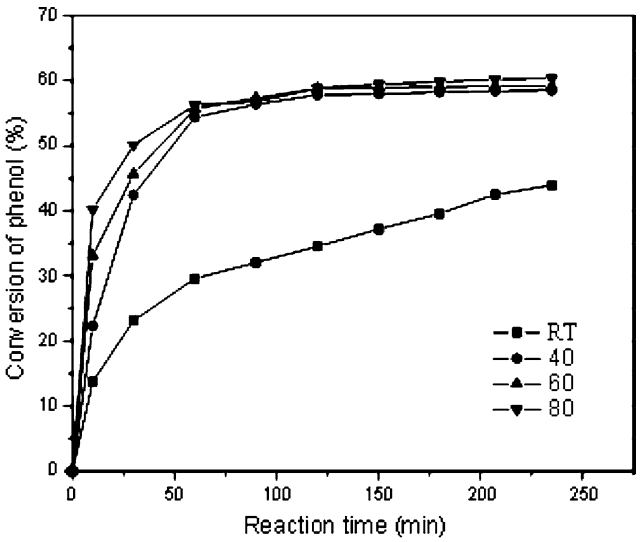

Fig. 8 Effect of time on stream on phenol conversion over Fe/Al-MCM-41 (25) at different temperatures

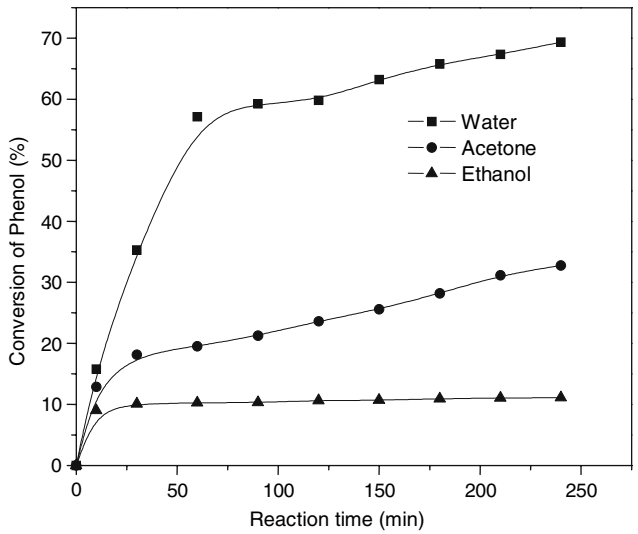

Fig. 9 Effect of solvents on phenol conversion over Fe/Al-MCM-41 (25)

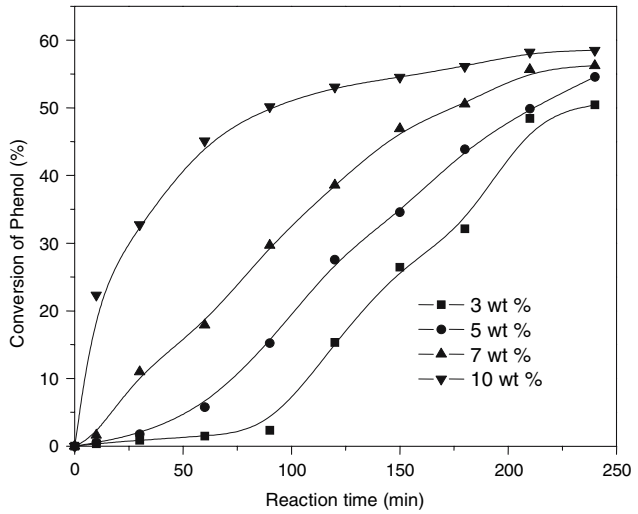

Fig. 10 Effect of Fe loading on Fe/Al-MCM-41 (25) on phenol conversion

3.2.6 Effect of % Fe content in Fe/AlMCM-41 (25)

Fe/Al-MCM-41 (25) catalysts were prepared with varying amounts of Fe from 3 wt% to 10 wt% and the corresponding reaction profile is shown in Fig. 10. Induction period was found strongly dependent on the amount of Fe species in the catalyst. Because with Comparatively less number of active sites it takes longer to activate hydrogen peroxide to form hydroxyl radical.

4 Conclusion

As the aluminium content in the Al-MCM-41 support material increases the incorporation of impregnated iron in the framework of Al-MCM-41 in Fe (10 wt%)/Al-MCM-41 increases as known from the d spacing and lattice parameter value of XRD analysis. Increase of aluminium content in the Al-MCM-41 support material increases the acidity of the Fe/Al-MCM-41 catalyst. The hydrophilic property of Fe/Al-MCM-41 plays a significant role in switching the selectivity towards hydroquinone and avoiding the strong adsorption of phenol and dihydroxy benzenes on Lewis acid site which can lead to coke formation and further undesired reaction like formation of tarry product and benzoquinone. As the acidity of the synthesized catalyst increases the percentage conversion of phenol also increases. The reported Fe/Al-MCM-41 catalysts requires very less induction period for the title reaction. Fe/MOR is found to be not suitable for the title reaction owing to the diffusional constraint offered by its small pores.

References

1. Lin S, Zhen Y, Wang SM, Dai YM (2000) J Mol Catal A: Chem 156:113
2. Xiong CR, Chen QL, Lu WR, Gao HX, Lu WK, Gao Z (2000) Catal Lett 69:231
3. Huybrechts DRC, Buskens PL, Jacobs PA (1992) J Mol Catal A: Chem 71:129
4. Dai P-SE, Petty RH, Ingram CW, Szostak R (1996) Appl Catal A: Gen 143:101
5. Maurya MR, Titinchi SJJ, Chand S, Mishra IM (2002) J Mol CatalA: Chem 180:201
6. Parvulescu V, Su BL (2001) Catal Today 69:315
7. Wang Y, Zhang Q, Shishido T, Takehira K (2002) J Catal 209:186
8. Norman H, Stuckyand GD, Tolman CA (1986) J Chem Soc Chem Commun 1521
9. Nakamuura M, Tatsumi T, Tominaga H (1990) Bull Chem Soc Jpn 63:3334
10. Villa AL, Caro CA, Correa CM (2005) J Mol Catal A:Chem 228:233
11. Selli E, Rossetti I, Meloni D, Sini F, Forni L (2004) Appl Catal A: Gen 262:131
12. Beck JS, Vartuli JC, Roth WJ, Leonowicz ME, Kresge CT, Schmitt KD, Chu CT-W, Olson DH, Sheppard EW, McCullen SB, Higgins JB, Schlenker JL (1992) J Am Chem Soc 114:10834
13. Sheldon RA, Arends IWCE, Lempers HEB (1998) Catal Today 41:387
14. Lee CW, Ahn DH, Wang B, Wang JSH, Park S (2001) Micro Meso Mater 44–45:587
15. Liu H, Lu G, Guo Y, Guo Y, Wang J (2006) Nanotechnology 17:997
16. Lou L, Liu S (2005) Catal Commun 6:762
17. Choi JS, Yoon SS, Jang SH, Ahn WS (2006) Catal Today 111:280
18. Decyk P, Trejda M, Ziolek M (2005) Chimie CR 8:635
19. Trejda M, Kujawa J, Ziolek M (2006) Catal Lett 108:141
20. Selvaraj M, Pandurangan A, Seshadri KS, Sinha PK, Krishnasamy V, Lal KB (2002) J Mol Catal A: Chem 186:173
21. Decyk P, Trejda M, Ziolek M, Glaszczka K, Bettahar M, Monteverdi S, Mercy M (2003) J Catal 219:146
22. Luan ZH, He H, Zhou WZ, Klinowski J (1998) J Chem Soc Faraday Trans 94:979

23. Climent MJ, Corma A, Iborra S, Miques S, Primo J, Rey F (1999) J Am Chem Soc 121:883
24. Climent MJ, Corma A, Iborra S, Miques S, Primo J, Rey F (1999) J Catal 183:76
25. Greggand SJ, Sing KSW (1982) Adsorption, surface area and porosity. second ed, Academic Press, New York
26. Emies CA (1993) J Catal 141:347
27. Samanta S, Giri S, Sastry PU, Mal NK, Manna A, Bhaumil A (2003) Ind Eng Chem Res 42:3012
28. Li Y, Feng Zh, Lian Y, Sun K, Zhang L, Jia G, Yang Q, Li C (2005) Micro Meso Mater 84:41
29. Hensen EJM, Zhu Q, Hendrix RM, Overweg AR, Kooyman PJ, Sychev MV, van Santen RA (2004) J Catal 221:560
30. Tippins HH (1970) Phys Rev B 1:126
31. Borgiga S, Buzzoni R, Geobaldo F, Lamberti C, Giamello E, Zecchina A, Leofanti G, Petrini G, Tozzola G, Vlaic G (1996) J Catal 158:486
32. Kuang Y, He N, Wang J, Xiao P, Yuan C, Lu Z (2001) Colloids Surf A 179:177
33. Dubey A, Rives V, Kannan S (2002) J Mol Catal A: Chem 181:151
34. Liu C, Shan Y, Yang X, Ye X, Wu Y (1997) J Catal 168:35
35. Mohamed MM, Eissa NA (2003) Mater Res Bull 38:1993
36. Tuel A, Moussa-Khouzami S, Taarit YB, Naccache C (1991) J Mol Catal A: Chem 68:45